

Crystallization kinetics, mechanical properties, and hydrolytic degradation of novel eco-friendly poly(butylene diglycolate) containing ether linkages

Feiyuan Jiang, Zhaobin Qiu

State Key Laboratory of Chemical Resource Engineering, MOE Key Laboratory of Carbon Fiber and Functional Polymers, Beijing University of Chemical Technology, Beijing 100029, China

Correspondence to: Z. Qiu (E-mail: qiuzb@mail.buct.edu.cn)

ABSTRACT: The basic thermal properties, isothermal melt crystallization kinetics, spherulitic morphology, mechanical properties, and hydrolytic degradation behavior of a novel eco-friendly polyester poly(butylene diglycolate) (PBDG) containing ether linkages were systematically studied with several techniques in this research. PBDG is an aliphatic polyester with high thermal stability. It had a glass transition temperature (T_g) of -25.7°C , a melting point temperature of 65.1°C , and an equilibrium melting point of 73.2°C . During the isothermal melt crystallization, PBDG crystallized slowly with increasing crystallization temperature, but the crystallization mechanism did not change. Negative spherulites were observed for PBDG. The mechanical properties of PBDG were investigated from the tensile testing. As a ductile polyester, PBDG possessed good mechanical properties. PBDG also showed a fast hydrolytic degradation rate. © 2016 Wiley Periodicals, Inc. *J. Appl. Polym. Sci.* **2016**, *133*, 44186.

KEYWORDS: crystallization; degradation; mechanical properties; thermal properties

Received 16 May 2016; accepted 14 July 2016

DOI: 10.1002/app.44186

INTRODUCTION

The excessive consumption of nondegradable polymeric materials has resulted in serious pollution to the environment. Therefore, the research and development of degradable polymeric materials are necessary and essential from an environmentally friendly viewpoint. Some biodegradable polyesters have been extensively reported, such as poly(L-lactide) (PLLA), poly(butylene succinate) (PBS), poly(ethylene succinate) (PES), poly(ethylene adipate) (PEA), and poly(butylene adipate) (PBA).^{1–14} In general, the backbone chains of these aliphatic polyesters consist of methylene ($-\text{CH}_2-$) and ester ($-\text{COO}-$) groups; moreover, most of these polyesters present slow crystallization rate, inferior mechanical properties, and slow degradation rate.^{4–14} Among them, PBS is an important biodegradable aliphatic polyester, which has been industrialized and extensively investigated.^{5–11} To develop new aliphatic polyesters with desired properties, some aliphatic polyesters containing ether linkages have attracted more and more interests.^{15–24} These polyesters have already been synthesized from some monomers with oxygen atom groups between dicarboxylic acids or diols; furthermore, they may be considered as potential degradable polymeric materials because of their chemical structures, thereby finding end use as agricultural ground films, compostable materials, biomedical materials, and disposable packing materials, etc.^{15–20}

In recent years, the synthesis and physical properties of poly(diethylene glycol succinate) (PDEGS), poly(triethylene dodecanoate) (PTED), and poly(butylene diglycolate) (PBDG) containing ether linkages have been reported in literature.^{19–23} It should be emphasized that all of these polyesters are highly hydrophilic and flexible. Cao *et al.* reported that PDEGS was synthesized through a polycondensation from diethylene glycol and succinic acid.²³ They found that PDEGS exhibited a completely amorphous feature and inferior thermal stability. The amorphous morphology was attributed to the chemical structure of diethylene glycol succinate (DEGS) unit. The ether structural moiety in DEGS segment completely inhibited PDEGS from crystallizing; moreover, the inferior thermal stabilities were also caused by the introduction of ether linkages. Genovese *et al.* synthesized PTED from 1,12-dodecanedioic acid and triethylene glycol, and found that PTED possessed high hydrophilicity, fast degradation rate, and good flexibility.¹⁹

The synthesis, characterization, and mechanical properties of PBDG has been investigated recently.^{20–22} In literature, Gigli *et al.* reported that PBDG was synthesized from dimethyldiglycolate and 1,4-butanediol via a transesterification process.²¹ They found that the melting temperature and glass transition temperature (T_g) of PBDG were 66°C and -23°C , respectively. They also studied the mechanical properties and crystal

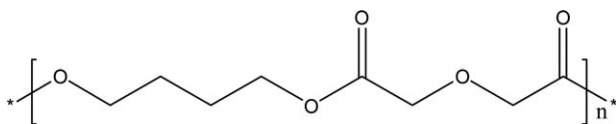


Figure 1. Chemical structure of PBDG.

structure of PBDG. PBDG presented a sharp crystalline diffraction peak at 19.38° and some other relatively weak diffraction peaks at 13.88° , 22.08° , 23.98° , 25.58° , and 26.68° . Furthermore, the stress and deformation at break were 23 MPa and 427%, respectively, and the Young's modulus of PBDG was 148 MPa. From the study of hydrophilic performance, the water contact angle of PBDG was 76° . The high hydrophilicity was due to the presence of highly electronegative ether-oxygen atoms along the PBDG chains.²⁰ In addition, they studied the nonisothermal melt crystallization behavior of PBDG. After the cooling process at $5^\circ\text{C}/\text{min}$ from the melt and the reheating process at $20^\circ\text{C}/\text{min}$, the crystallization exothermic peak and melting endothermic peak of PBDG under investigation were not observed. Moreover, they did not appear even at $1^\circ\text{C}/\text{min}$, indicating its weak crystallization ability.²²

In this work, PBDG was synthesized from diglycolate acid (DGA) and butanediol (BDO) through a melt polycondensation method.^{25,26} Moreover, we systematically studied the thermal properties, isothermal melt crystallization kinetics, crystalline morphology, mechanical properties, and hydrolytic degradation behavior of PBDG. The importance of this work was as follows. First, it would be a complete research about PBDG, because we reported the isothermal melt crystallization kinetics, crystalline morphology, and degradation behavior of PBDG for the first time. Second, it may provide a reference for the further study of other aliphatic polyesters containing ether linkages. Third, it was essential for the future research to develop new PBDG-based multicomponent degradable materials through copolymerization and blending. Fourth, this work may be of interest and help for the wider application of PBDG from a practical viewpoint.

EXPERIMENTAL

Materials and Synthesis of PBDG

The monomers diglycolate acid (DGA) and butanediol (BDO) were bought from Alfa Aesar Chemicals Co. Ltd. and Tianjin Fu Chen Chemical Reagent Factory, respectively, and the catalyst tetrabutyl titanate was bought from Beijing Chang Ping Jing Xiang Chemical Factory.

PBDG was synthesized from the condensation of DGA and BDO through a typical two-step melt polycondensation method (esterification and polycondensation).^{25,26} For brevity, the detailed synthesis process was not described here. The chemical structure of PBDG is shown in Figure 1.

CHARACTERIZATIONS

The number-average and weight-average molecular weights of the synthesized sample in this research were 3.73×10^4 and 5.14×10^4 g/mol, respectively, which were measured by a gel

permeation chromatography (GPC) (Agilent 2006 Series, Santa Clara, California), using dimethylformamide as the solvent.

A thermogravimetric analysis (TGA) (TA Instruments Q50, New Castle, Delaware) was used to study the thermal stability of PBDG from room temperature to 580°C at $20^\circ\text{C}/\text{min}$ under nitrogen atmosphere with a nitrogen flow of 50 mL/min. The weight of the PBDG sample in powder form was around 4 mg for the TGA measurement.

The basic thermal parameters and crystallization behaviors were investigated by a differential scanning calorimeter (DSC) (TA Instruments DSC Q100, New Castle, Delaware) with a nitrogen flow of 50 mL/min. For each DSC test, a fresh sample of around 5 mg was used in this work. To study the basic thermal parameters [glass transition temperature (T_g) and melting temperature (T_m)], the sample was heated from 20 to 100°C at $10^\circ\text{C}/\text{min}$ (first heating), held at 100°C for 3 min to eliminate any previous thermal history, cooled to -80°C at $60^\circ\text{C}/\text{min}$, and reheated to 100°C at $10^\circ\text{C}/\text{min}$ (second heating). The isothermal melt crystallization kinetics was also investigated. PBDG was cooled from the crystal-free melt to the chosen crystallization temperature (T_c) at $60^\circ\text{C}/\text{min}$ and held for a enough long time until no further obvious change of heat flow with time could be detected to ensure complete crystallization. Based on the recorded exothermic curves of heat flow as a function of time, relative crystallinity (X_t) at crystallization time (t) could be calculated by the following equation:

$$X_t = \frac{\int_{t_0}^t \left(\frac{dH_c}{dt} \right) dt}{\int_{t_0}^{t_\infty} \left(\frac{dH_c}{dt} \right) dt} \quad (1)$$

where dH_c/dt was the rate of heat evolution, and t_0 and t_∞ were the onset and end time of crystallization time, respectively. For the estimation of equilibrium melting point, PBDG was first crystallized in an oven at different T_c values for 12 h and then scanned with DSC to study the subsequent melting behavior at $10^\circ\text{C}/\text{min}$.

The crystalline morphology of PBDG was investigated with a polarized optical microscope (POM) (Olympus BX51, Tokyo, Japan) with a Linkam THMS600 temperature controller.

The mechanical properties of PBDG were investigated with a universal tensile machine (Instron 1185, Norwood, America) with a rate of 50 mm/min at 25°C . Before quenching into ice water, PBDG was first pressed into film at 105°C for 10 min with a homemade hot pressing machine. Five dumbbell shaped specimens with dimensions of $40 \text{ mm} \times 4 \text{ mm} \times 0.5 \text{ mm}$ were tested for PBDG under identical conditions, and then the average of these values was taken.

For the hydrolytic degradation study, the samples were washed with deionized water and dried in a vacuum at 25°C to reach a constant weight after degradation in a sodium hydroxide (NaOH) solution ($\text{pH} = 14$) at 37°C for different periods of time from 2 to 16 h with an interval of 2 h. The hydrolytic degradation rate of PBDG was determined by the variation of weight loss with degradation time. The weight loss coefficient

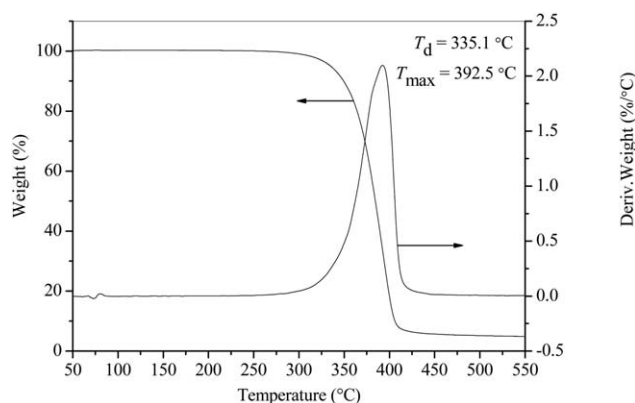


Figure 2. TGA results of PBDG.

(W_{loss}) was calculated by the following relationship: $W_{\text{loss}} = (W_0 - W_{t\text{-dried}})/W_0$, where W_0 was the initial weight and $W_{t\text{-dried}}$ was the weight of the sample undergoing a hydrolytic degradation time t and drying in vacuum. Moreover, the hydrolytic degradation rate (R) was determined by the following relationship: $R = dW_{\text{loss-}t}/dt$.

A scanning electron microscope (SEM) (JEOL JSM-7800F, Tokyo, Japan) was used to observe the surfaces of PBDG film before and after the hydrolytic degradation. The SEM images were obtained under 2,000 times magnification with a voltage of 2 kV. The films were coated with gold before observation.

RESULTS AND DISCUSSION

Basic Thermal Behavior of PBDG

It is essential to investigate the thermal stability of PBDG, as it may affect the processing condition from a practical viewpoint. Figure 2 illustrates the thermal stability results of PBDG. PBDG displayed a thermal decomposition temperature at 5 wt % weight loss (T_d) of 335.1 °C and a temperature at the maximum degradation rate (T_{max}) of 392.5 °C. Gigli *et al.* reported that PBDG had a T_d of 330 °C, and PBS had a T_d of 305 °C.^{21,22} Therefore, the thermal stability of the synthesized PBDG sample in this work was comparable to that of the sample reported by Gigli *et al.*; moreover, PBDG had a higher thermal stability than PBS.

As introduced in the Experimental section, the glass transition temperature (T_g) and melting temperature (T_m) of PBDG were measured with DSC. When PBDG was heated from the amorphous state (second heating), the crystallization of PBDG did not occur; therefore, T_m of PBDG could not be read from the second heating process. In this work, T_m of PBDG was determined from the first heating DSC trace on the as synthesized sample, while T_g was read from the second heating process on the amorphous sample after cooling from the melt. Figure 3(a) shows that PBDG had a T_m of 65.1 °C, while Figure 3(b) displays that T_g of PBDG was -25.7 °C. From Figure 3(a), the heat of fusion of PBDG was measured to be 68.7 J/g. The obtained T_g and T_m values of PBDG in this work were very close to those reported by Gigli *et al.* (-27 °C for T_g and 66 °C for T_m).²¹

The subsequent melting behaviors of PBDG after crystallizing at different T_c values were further investigated by DSC. Figure 4 displays the melting behaviors of PBDG after isothermally

crystallizing from 35 to 50 °C. PBDG was crystallized for 12 h at different T_c values to ensure the sufficient crystallization and avoid the influence of crystallization time. As illustrated in Figure 4, PBDG showed an evident single melting endotherm, which gradually shifted upwards to high temperature range with increasing T_c . The shift of the melting endotherm to high temperature range with increasing T_c was reasonable from a polymer crystallization viewpoint, because the thickness of the crystals formed at higher T_c was greater than that of the crystals formed at lower T_c . Therefore, the relatively thicker and more perfect crystals would undergo melting later than the thinner and imperfect crystals. Accordingly, the melting endotherm was found to shift to high temperature range with an increase in T_c .

In this work, the equilibrium melting point temperature (T_m^0) of PBDG was calculated by the Hoffman–Weeks equation, which is described as follows:

$$T_m = \eta T_c + (1 - \eta) T_m^0 \quad (2)$$

where T_m^0 represents the equilibrium melting point and η may be considered as a measure of the stability related to the crystal

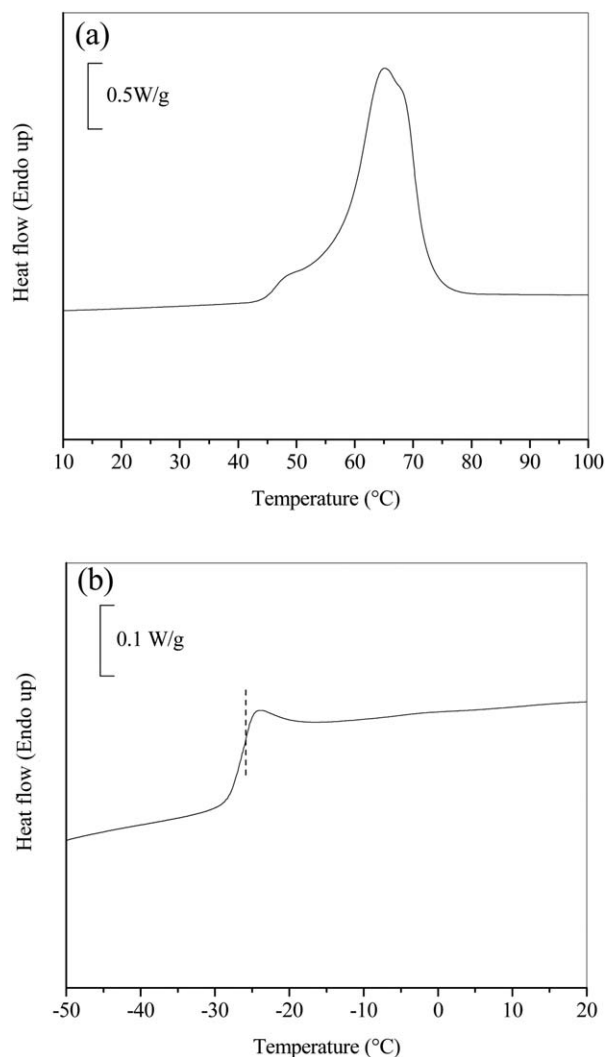


Figure 3. DSC curves of PBDG showing (a) melting endotherm and (b) glass transition region.

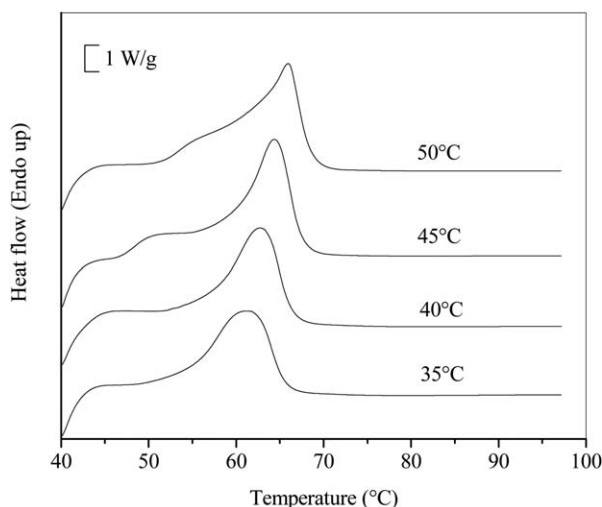


Figure 4. Melting behaviors of PBDG after crystallizing at indicated T_c values.

layer thickness of the polymer.²⁷ Figure 5 displays the Hoffman–Weeks plot of PBDG. T_m^0 was calculated as 73.2 °C and η was 0.31.

Isothermal Melt Crystallization Kinetics of PBDG

The isothermal melt crystallization kinetics of PBDG was also studied by DSC. Figure 6(a) describes the evolution of relative crystallinity (X_t) with crystallization time (t) of PBDG at indicated T_c values. From Figure 6(a), crystallization time became longer with an increase in T_c , indicating that the isothermal melt crystallization of PBDG was retarded. Such result was reasonable from a viewpoint of polymer crystallization, as the degree of supercooling ($\Delta T = T_m^0 - T_c$) became smaller with an increase in T_c ; therefore, the driving force for the sample to crystallize (including nucleation and crystal growth) also became smaller. Consequently, it was more difficult for the sample to complete crystallization at higher T_c than at lower T_c when the sample was isothermally crystallized from the melt, thereby prolonging crystallization time with an increase in T_c .

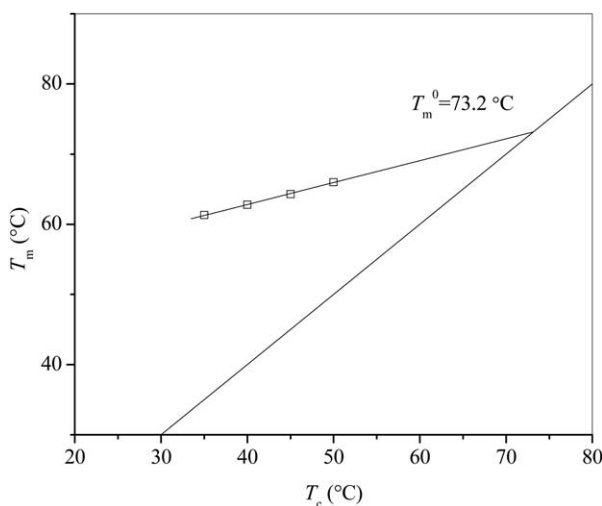


Figure 5. The Hoffman–Weeks plot of PBDG.

The well-known Avrami equation was used to analyze the isothermal melt crystallization kinetics of PBDG, which is shown as follows:

$$1 - X_t = \exp(-kt^n) \quad (3)$$

where n is the Avrami exponent and k is the crystallization rate constant.^{28,29} The Avrami plots of PBDG at different T_c values are displayed in Figure 6. As illustrated in Figure 6, five almost parallel lines were acquired for PBDG, indicating the applicability of the Avrami equation for fitting the isothermal melt crystallization process and the unchanged crystallization mechanism of PBDG.

The obtained n and k values are summarized in Table I for comparison. In the wide T_c range, the n values of PBDG slightly varied from 2.7 to 2.8. Regardless of T_c , all the n values were roughly constant, suggesting the same crystallization mechanism, i.e., a three-dimensional spherulitic growth with athermal nucleation mechanism³⁰; furthermore, the k values accordingly decreased with an increase of T_c . For example, when PBDG was crystallized at 20, 23, and 26 °C, the k values were 1.02×10^{-4} , 0.71×10^{-4} , and $3.80 \times 10^{-5} \text{ min}^{-2.8}$, respectively.

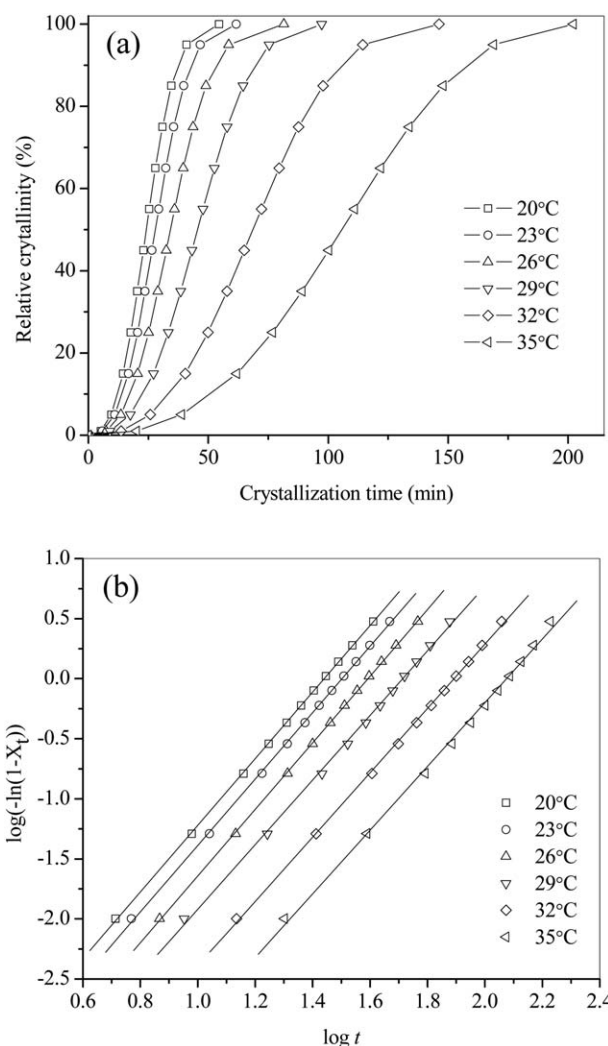
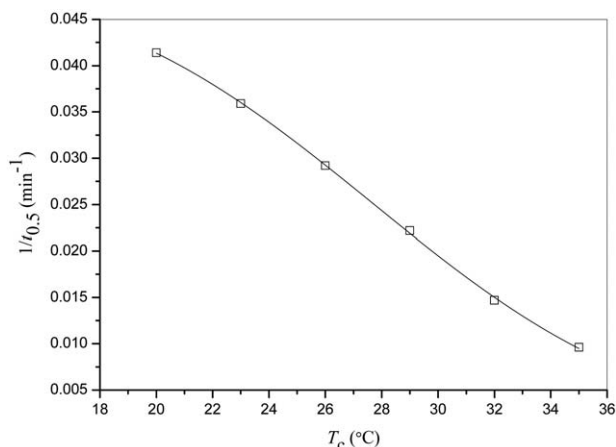


Figure 6. (a) X_t-t plots and (b) Avrami plots of PBDG.

Table I. Isothermal Melt Crystallization Kinetics Parameters of PBDG

T_c (°C)	n	k (min ⁻ⁿ)
20	2.77 ± 0.01	$(1.02 \pm 0.03) \times 10^{-4}$
23	2.76 ± 0.02	$(7.05 \pm 0.43) \times 10^{-5}$
26	2.77 ± 0.01	$(3.82 \pm 0.15) \times 10^{-5}$
29	2.69 ± 0.03	$(2.46 \pm 0.30) \times 10^{-5}$
32	2.68 ± 0.02	$(8.54 \pm 0.81) \times 10^{-6}$
35	2.65 ± 0.04	$(3.15 \pm 0.63) \times 10^{-6}$

**Figure 7.** Plot of $1/t_{0.5}$ versus T_c for PBDG.

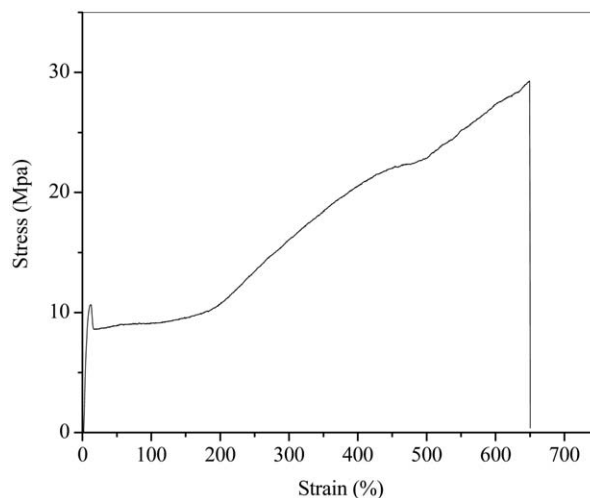
To further discuss the crystallization melt kinetics of PBDG, the crystallization half-time ($t_{0.5}$) value, the time at 50% of the final crystallinity of the sample, was acquired through the following equation:

$$t_{0.5} = \left(\frac{\ln 2}{k} \right)^{1/n} \quad (4)$$

The reciprocal of $t_{0.5}$ ($1/t_{0.5}$) could be used to represent the crystallization rate; therefore, Figure 7 illustrates the plot of $1/t_{0.5}$ versus T_c . As clearly shown in Figure 7, the values of $1/t_{0.5}$ decreased with increasing T_c , indicating that PBDG crystallized more slowly as the degree of supercooling became smaller.

The Crystalline Morphology of PBDG

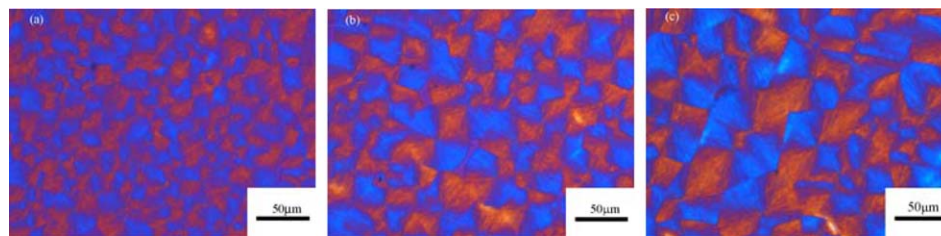
The mechanical properties and degradability of aliphatic polyesters are directly related to the crystalline morphology. Therefore, the crystalline morphology of PBDG was further

**Figure 9.** Stress–strain curve of PBDG.

investigated with POM. Figure 8 presents the characteristic spherulitic morphology of PBDG after crystallizing at 28, 30, and 32 °C. All the negative spherulites of PBDG impinged with each other and filled the whole field of the observation; moreover, the spherulites boundaries were relatively clear, especially at high crystallization temperature. In addition, with increasing crystallization temperature, the nucleation density of PBDG spherulites gradually decreased, resulting in the bigger size of the spherulites at high crystallization temperature.

Mechanical Properties of PBDG

It is important to investigate the mechanical properties of PBDG for its practical application. The typical stress–strain curve of PBDG is displayed in Figure 9. From Figure 9, the following conclusions were obtained. First, PBDG exhibited an obvious yield behavior with yield strength of 10.6 ± 1.0 MPa at the strain of about $12 \pm 2.0\%$. Second, the Young's modulus of PBDG was determined to be 166.4 ± 20 MPa. Third, the final elongation at break of PBDG was estimated to be about $650 \pm 30\%$ with a tensile strength of 29.3 ± 2.0 MPa. It was interesting to note that the mechanical properties of PBDG in this work were comparable to and even slightly better than those reported by Gigli *et al.*²¹ The slight improvement of the mechanical properties of PBDG in this research may arise from its relatively high molecular weight. In this research, PBDG had a number-average molecular weight of 3.73×10^4 g/mol, while that of the PBDG sample synthesized by Gigli *et al.* was $2.81 \times$

**Figure 8.** PBDG spherulites after crystallizing at (a) 28 °C, (b) 30 °C, and (c) 32 °C. [Color figure can be viewed in the online issue, which is available at wileyonlinelibrary.com.]

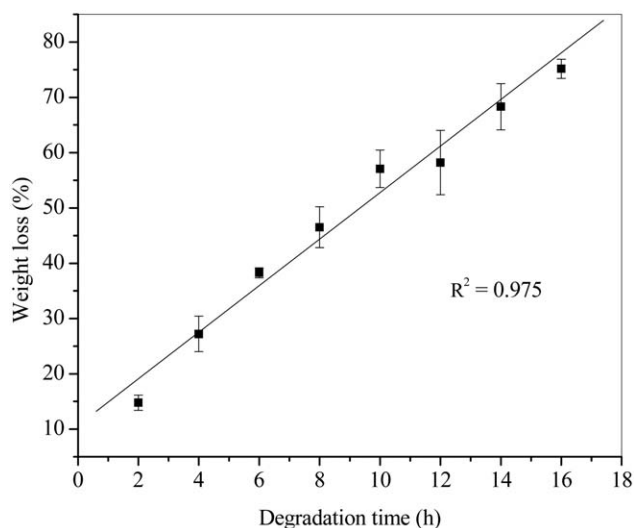


Figure 10. Plot of weight loss of PBDG versus hydrolytic degradation time in a NaOH solution.

10^4 g/mol.²¹ Therefore, the relatively high molecular weight of PBDG in this work displayed better mechanical properties. It should also be noted that the mechanical properties of PBDG was related to the crystallinity value of the sample. In this work, the crystallinity for the tensile testing was around 30%. In brief, PBDG is a ductile polyester with good mechanical properties, which may be used as a novel eco-friendly polymeric material from a practical viewpoint.

Hydrolytic Degradation of PBDG

Similar to other aliphatic polyesters, PBDG may also undergo degradation; therefore, the study of the hydrolytic degradation behavior of PBDG is interesting and important from both the academic and practical viewpoints. The hydrolytic degradation of PBDG was studied in a NaOH solution (pH = 14) at 37 °C. Figure 10 illustrates the plot of the weight loss of PBDG versus hydrolytic degradation time, showing the increased weight loss with prolonging hydrolytic degradation time. As a result, PBDG lost about 80% of its original weight after only a degradation time of 16 h. From the slope of the plot of the weight loss versus degradation time, the degradation rate was determined to be around 5%/h, which was greater than those of other aliphatic polyesters without heteroatoms in the backbone chains. For instance, poly(butylene suberate) (PBSub) lost its 80% weight

within around 3 days under the same experimental condition,³¹ suggesting that PBSub degraded more slowly than PBDG.

The surface morphologies of the original and degraded PBDG films were further investigated with SEM. As shown in Figure 11(a), the surface of the PBDG film before hydrolytic degradation was smooth. As demonstrated in Figure 11(b), the surface of the film after a hydrolytic degradation of 16 h became rougher. In addition, many irregular holes were observed for the film after the hydrolytic degradation. These changes demonstrated that PBDG degraded rapidly within a short time period.

CONCLUSIONS

In the present work, a novel eco-friendly aliphatic polyester PBDG with high molecular weight was successfully synthesized from diglycolate acid and butanediol through a typical two-step melt polycondensation method. The thermal properties, isothermal melt crystallization kinetics, mechanical properties, and hydrolytic degradation of PBDG were systematically studied. PBDG showed a high thermal stability. PBDG had a glass transition temperature of -25.7 °C, a melting point temperature of 65.1 °C, and an equilibrium melting point of 73.2 °C. The Avrami method was applied to fit the isothermal melt crystallization kinetics of PBDG within the investigated crystallization temperature range. Regardless of crystallization temperature, the Avrami exponent values varied slightly and were close to 3, indicating the same crystallization mechanism. Negative spherulites were observed for PBDG after isothermal melt crystallization. The mechanical properties of PBDG were also investigated from the tensile testing. PBDG exhibited an obvious yield behavior at a small strain range; moreover, the Young's modulus, elongation at break, and tensile strength values of PBDG were determined. PBDG possessed good mechanical properties; especially, it had a great elongation at break value, which may make it a good candidate as a ductile aliphatic polyester in some practical application fields. In addition, PBDG degraded quickly in a NaOH solution, indicating that it may find end use as a degradable material. From the promising performance, PBDG may not only be used as a novel kind of environmentally friendly polymeric material but also be extended to polymer blending to develop new degradable materials with desirable properties.

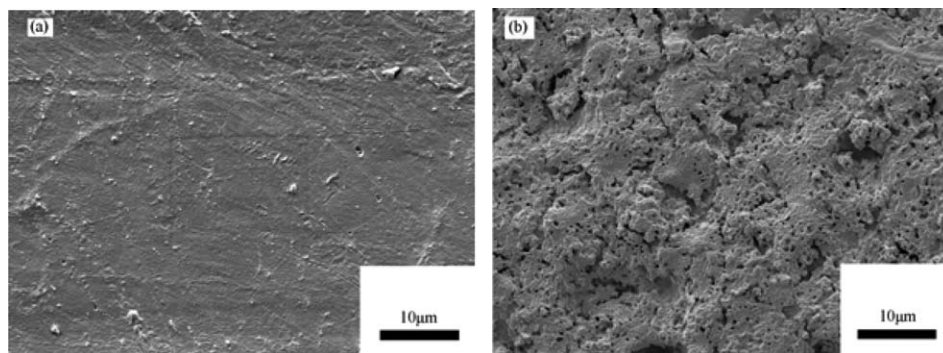


Figure 11. The SEM images of PBDG showing the surface morphologies; (a) before and (b) after degradation.

ACKNOWLEDGMENTS

Part of this work was supported by the National Natural Science Foundation, China (51373020, 51573016, and 51521062).

REFERENCES

1. Tsuji, H. *Macromol. Biosci.* **2005**, *5*, 569.
2. Shibata, M.; Inoue, Y.; Miyoshi, M. *Polymer* **2006**, *47*, 3557.
3. Qiu, Z.; Pan, H. *Compos. Sci. Technol.* **2010**, *70*, 1089.
4. Qiu, Z.; Zhou, P. *RSC Adv.* **2014**, *4*, 51411.
5. Sinha Ray, S.; Okamoto, K.; Okamoto, M. *Macromolecules* **2003**, *36*, 2355.
6. Du, X.; Xu, X.; Liu, X.; Yang, J.; Wang, Y.; Gao, X. *Polym. Degrad. Stab.* **2016**, *123*, 94.
7. Papageorgiou, G.; Achilias, S.; Bikiaris, D. *Macromol. Chem. Phys.* **2007**, *208*, 1250.
8. Wang, G.; Qiu, Z. *Ind. Eng. Chem. Res.* **2012**, *51*, 16369.
9. Xu, J.; Guo, B. *Biotechnol. J.* **2010**, *5*, 1149.
10. Qiu, Z.; Komura, M.; Ikehara, T.; Nishi, T. *Polymer* **2003**, *44*, 7781.
11. Gan, Z.; Abe, H.; Kurokawa, H.; Doi, Y. *Biomacromolecules* **2001**, *2*, 605.
12. Li, X.; Qiu, Z. *RSC Adv.* **2015**, *5*, 103713.
13. Wu, H.; Qiu, Z. *Ind. Eng. Chem. Res.* **2012**, *51*, 13323.
14. Zhao, Y.; Qiu, Z. *Cryst. Eng. Comm.* **2011**, *13*, 7129.
15. Gigli, M.; Lotti, N.; Gazzano, M.; Siracusa, V.; Finelli, L.; Munari, A.; Rosa, M. D. *Polym. Degrad. Stab.* **2014**, *105*, 96.
16. Gigli, M.; Lotti, N.; Vercellino, M.; Visai, L.; Munari, A. *Mater. Sci. Eng., C* **2014**, *34*, 86.
17. Ding, M.; Zhang, M.; Yang, J.; Qiu, J. *Biodegradation* **2012**, *23*, 127.
18. Gigli, M.; Negroni, A.; Soccio, M.; Zanaroli, G.; Lotti, N.; Fava, F.; Munari, A. *Green Chem.* **2012**, *14*, 2885.
19. Genovese, L.; Gigli, M.; Lotti, N.; Gazzano, M.; Siracusa, V.; Munari, A.; Rosa, M. D. *Ind. Eng. Chem. Res.* **2014**, *53*, 10965.
20. Gigli, M.; Lotti, N.; Gazzano, M.; Siracusa, V.; Finelli, L.; Munari, A.; Rosa, M. D. *Ind. Eng. Chem. Res.* **2013**, *52*, 12876.
21. Gigli, M.; Lotti, N.; Gazzano, M.; Finelli, L.; Munari, A. *React. Funct. Polym.* **2012**, *72*, 303.
22. Gigli, M.; Lotti, N.; Gazzano, M.; Finelli, L.; Munari, A. *Polym. Eng. Sci.* **2013**, *53*, 491.
23. Cao, A.; Okamura, T.; Nakayama, K.; Inoue, Y.; Masuda, T. *Polym. Degrad. Stab.* **2002**, *78*, 107.
24. Chen, H.; Gigli, M.; Gualandi, C.; Truckenmüller, R.; van Blitterswijk, C.; Lotti, N.; Munari, A.; Focarete, M. L.; Moroni, L. *Biomaterials* **2016**, *76*, 261.
25. Wu, H.; Qiu, Z. *Cryst. Eng. Comm.* **2012**, *14*, 3586.
26. Yang, Y.; Qiu, Z. *Cryst. Eng. Comm.* **2011**, *13*, 2408.
27. Hoffman, J. D.; Weeks, J. J. *J. Chem. Phys.* **1965**, *42*, 4301.
28. Avrami, M. *J. Chem. Phys.* **1940**, *8*, 212.
29. Avrami, M. *J. Chem. Phys.* **1941**, *9*, 177.
30. Wunderlich, B. In *Macromolecular Physics*; Academic Press: New York, **1976**; Vol. 2, p 147.
31. Cui, Z.; Qiu, Z. *Polymer* **2015**, *67*, 12.